Article

Preparation and Controlled Self-Assembly of Janus Magnetic Nanoparticles

Marco Lattuada, and T. Alan Hatton

J. Am. Chem. Soc., **2007**, 129 (42), 12878-12889• DOI: 10.1021/ja0740521 • Publication Date (Web): 02 October 2007

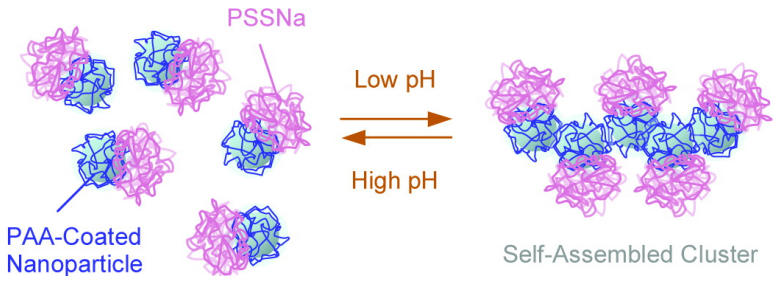

More About This Article

Additional resources and features associated with this article are available within the HTML version:

- Supporting Information
- Links to the 11 articles that cite this article, as of the time of this article download
- Access to high resolution figures
- Links to articles and content related to this article
- Copyright permission to reproduce figures and/or text from this article

View the Full Text HTML

J|A|C|S
ARTICLES
Published on Web 10/02/2007

Preparation and Controlled Self-Assembly of Janus Magnetic Nanoparticles

Marco Lattuada† and T. Alan Hatton*

Contribution from the Department of Chemical Engineering, Massachusetts Institute of Technology, 77 Massachusetts Avenue, Cambridge, Massachusetts 02139

Received June 30, 2007; E-mail: tahatton@mit.edu

Abstract: Janus magnetic nanoparticles (~20 nm) were prepared by grafting either polystyrene sodium sulfonate (PSSNa) or polydimethylamino ethylmethacrylate (PDMAEMA) to the exposed surfaces of negatively charged poly(acrylic acid) (PAA)-coated magnetite nanoparticles adsorbed onto positively charged silica beads. Individually dispersed Janus nanoparticles were obtained by repulsion from the beads on reversal of the silica surface charge when the solution pH was increased. Controlled aggregation of the Janus nanoparticles was observed at low pH values, with the formation of stable clusters of approximately 2−4 times the initial size of the particles. Cluster formation was reversed, and individually dispersed nanoparticles recovered, by restoring the pH to high values. At intermediate pH values, PSSNa Janus nanoparticles showed moderate clustering, while PDMAEMA Janus nanoparticles aggregated uncontrollably due to dipolar interactions. The size of the stable clusters could be controlled by increasing the molecular weight of the grafted polymer, or by decreasing the magnetic nanoparticle surface availability for grafting, both of which yielded larger cluster sizes. The addition of small amounts of PAA-coated magnetic nanoparticles to the Janus nanoparticle suspension resulted in a further increase in the final cluster size. Monte Carlo simulation results compared favorably with experimental observations and showed the formation of small, elongated clusters similar in structure to those observed in cryo-TEM images.

Introduction

Magnetic nanoparticles have attracted increasing interest in the material and colloid science communities in recent years.[1−19] Early investigations, over 40 years ago, targeted the fundamental properties of magnetic nanoparticles suspensions,[1,20] which soon found applications in magnetic ball bearings technology,[1] and in magnetorheological suspensions.[21,22] More recent research has been devoted to high-tech applications as in the fields of magnetic storage devices and of biomedical engineering and bioseparations.[13,18,19,23−28] The quest for substrates having extremely high magnetic storage capacities prompted the search for new recipes to prepare nanoparticles with highly controlled morphology and well-defined size distributions,[12,15,18] while others have focused on developing new techniques to control the surface functionalization of magnetic nanoparticles.[26,28−31]

† Present address: Institute for Chemical and Bioengineering, ETH Zurich, 8093 Zurich, Switzerland.

(1) Rosensweig, R. E. *Ferrohydrodynamics*; Dover Publications Inc.: Mineola, NY, 1985.
(2) Mikhailik, O. M.; Povstugar, V. I.; Mikhailova, S. S.; Lyakhovich, A. M.; Fedorenko, O. M.; Kurbatova, G. T.; Shklovskaya, N. I.; Chuiko, A. A. *Colloids Surf.* **1991**, *52*, 315−324.
(3) Wooding, A.; Kilner, M.; Lambrick, D. B. *J. Colloid Interface Sci.* **1991**, *144*, 236−242.
(4) Wooding, A.; Kilner, M.; Lambrick, D. B. *J. Colloid Interface Sci.* **1992**, *149*, 98−104.
(5) Kang, Y. S.; Risbud, S.; Rabolt, J. F.; Stroeve, P. *Chem. Mater.* **1996**, *8*, 2209−2211.
(6) Lefebure, S.; Dubois, E.; Cabuil, V.; Neveu, S.; Massart, R. *J. Mater. Res.* **1998**, *13*, 2975−2981.
(7) Holzwarth, A.; Lou, J. F.; Hatton, T. A.; Laibinis, P. E. *Ind. Eng. Chem. Res.* **1998**, *37*, 2701−2706.
(8) Shen, L. F.; Laibinis, P. E.; Hatton, T. A. *Langmuir* **1999**, *15*, 447−453.
(9) Shen, L. F.; Laibinis, P. E.; Hatton, T. A. *J. Magn. Magn. Mater.* **1999**, *194*, 37−44.
(10) Murray, C. B.; Sun, S. H.; Doyle, H.; Betley, T. *MRS Bull.* **2001**, *26*, 985−991.
(11) Pileni, M. P. *Adv. Funct. Mater.* **2001**, *11*, 323−336.
(12) Sun, S. H.; Zeng, H. *J. Am. Chem. Soc.* **2002**, *124*, 8204−8205.
(13) Bucak, S.; Jones, D. A.; Laibinis, P. E.; Hatton, T. A. *Biotechnol. Prog.* **2003**, *19*, 477−484.
(14) Sun, S. H.; Anders, S.; Thomson, T.; Baglin, J. E. E.; Toney, M. F.; Hamann, H. F.; Murray, C. B.; Terris, B. D. *J. Phys. Chem. B* **2003**, *107*, 5419−5425.
(15) Hyeon, T. *Chem. Commun.* **2003**, 927−934.
(16) Park, J.; An, K. J.; Hwang, Y. S.; Park, J. G.; Noh, H. J.; Kim, J. Y.; Park, J. H.; Hwang, N. M.; Hyeon, T. *Nat. Mater.* **2004**, *3*, 891−895.
(17) Moeser, G. D.; Green, W. H.; Laibinis, P. E.; Linse, P.; Hatton, T. A. *Langmuir* **2004**, *20*, 5223−5234.
(18) Sun, S. H.; Zeng, H.; Robinson, D. B.; Raoux, S.; Rice, P. M.; Wang, S. X.; Li, G. X. *J. Am. Chem. Soc.* **2004**, *126*, 273−279.
(19) Ditsch, A.; Lindenmann, S.; Laibinis, P. E.; Wang, D. I. C.; Hatton, T. A. *Ind. Eng. Chem. Res.* **2005**, *44*, 6824−6836.
(20) De Gennes, P. G.; Pincus, P. A. *Phys. Condens. Matter* **1970**, *11*, 189−198.
(21) Rankin, P. J.; Ginder, J. M.; Klingenberg, D. J. *Curr. Opin. Colloid Interface Sci.* **1998**, *3*, 373−381.
(22) Tao, R. *J. Phys.: Condens. Matter* **2001**, *13*, R979−R999.
(23) Moeser, G. D.; Roach, K. A.; Green, W. H.; Hatton, T. A.; Laibinis, P. E. *AIChE J.* **2004**, *50*, 2835−2848.
(24) Gonzales, M.; Krishnan, K. M. *J. Magn. Magn. Mater.* **2005**, *293*, 265−270.
(25) Ditsch, A.; Laibinis, P. E.; Wang, D. I. C.; Hatton, T. A. *Langmuir* **2005**, *21*, 6006−6018.
(26) Grancharov, S. G.; Zeng, H.; Sun, S. H.; Wang, S. X.; O'Brien, S.; Murray, C. B.; Kirtley, J. R.; Held, G. A. *J. Phys. Chem. B* **2005**, *109*, 13030−13035.
(27) Berry, C. C. *J. Mater. Chem.* **2005**, *15*, 543−547.
(28) Neuberger, T.; Schopf, B.; Hofmann, H.; Hofmann, M.; von Rechenberg, B. *J. Magn. Magn. Mater.* **2005**, *293*, 483−496.
(29) Xie, J.; Peng, S.; Brower, N.; Pourmand, N.; Wang, S. X.; Sun, S. H. *Pure Appl. Chem.* **2006**, *78*, 1003−1014.
(30) Jun, Y. W.; Huh, Y. M.; Choi, J. S.; Lee, J. H.; Song, H. T.; Kim, S.; Yoon, S.; Kim, K. S.; Shin, J. S.; Suh, J. S.; Cheon, J. *J. Am. Chem. Soc.* **2005**, *127*, 5732−5733.

10.1021/ja0740521 CCC: $37.00

The challenge is to find suitable procedures, recipes, and strategies to attach and/or grow polymers, biomolecules, or simple surfactants on the nanoparticle surface. The functionalization of nanoparticles, in general, is currently a most promising research topic in nanotechnology,[32−34] with the goal of tailoring particle properties at the nanoscale to attain an unprecedented level of control of their behavior.

The ability to control the self-assembly behavior of nanoparticles by means of advanced functionalization techniques to form clusters of desired size and with tunable properties has opened up a wide variety of possible applications.[33] In the case of magnetic nanoparticles, some effort has been devoted recently to the preparation of magnetic clusters of defined size, dictated by their responsiveness to magnetic fields in high gradient magnetic separation devices, for protein separations from fermentation broths.[25] These clusters are formed directly during the initial particle nucleation and growth phase in the synthesis, and their size can be controlled by carefully dosing the amount and timing of polymer addition necessary to stabilize the final clusters. Berret et al. have delineated the need for similar considerations in the development of new contrast agents for magnetic resonance imaging and controlled cluster formation by using coacervation of polyelectrolyte-neutral block copolymers with pre-prepared superparamagnetic nanoparticles.[35] Clusters formed in these ways are obviously irreversible in nature.

The preparation of particles that can be induced to form clusters with well-defined sizes reversibly in response to appropriate stimuli is a more challenging problem. Such clusters could find applications whenever size control is an issue and where the presence of clusters is only desirable under certain circumstances. An example is in high gradient magnetic separation processes, where the high surface areas of individually dispersed nanoparticles allow for high rates and capacities of adsorption or catalysis, but larger clusters are needed for efficient scavenging of the particles from the fluid phase once their job is done. However, the preparation of reversible clusters with a defined size requires a higher level of nanoparticle functionalization than is required in common cluster preparation procedures. Thus, there is a need to design and create the building blocks whose assembly will generate reversible clusters.

Janus particles can meet these needs. These particles are symmetric in shape but asymmetric in surface properties due to the distribution of different functional groups over the particle surfaces. Much effort has been devoted recently to the development of these particles[36−44] whose patchy surfaces strongly influence their overall behavior in terms of reactivity and colloidal stability. Recent computer simulations on Janus particles predict that appropriately designed patches can confer to the particles exotic self-assembly characteristics and peculiar phase transitions.[45−47] The development of suitable strategies to prepare Janus nanoparticles is, therefore, of great interest, even as it also presents serious challenges.

Recently, a number of techniques have been proposed for the asymmetric functionalization of particles and nanoparticles.[39] While some of these methods allow direct preparation of asymmetric particles,[41] in most cases a pre-prepared particle is functionalized on only a portion of its surface, either by masking or protecting a part of the particle surface, or by trapping the particle at the interface between two phases, so that only that part of the particle is exposed and available for chemical modification. To date, this procedure has been applied successfully to large particles, usually sub-micrometer to a few micrometers in size.[37,40] However, to fully exploit the capabilities offered by self-assembly, it is desirable to functionalize much smaller nanoparticles, on the order of a few nanometers. For this objective, other approaches need to be developed. For example, Gu et al.[48] have successfully created asymmetric nanoparticles by trapping them at the surfaces of emulsion droplets and carrying out a functionalization on the side facing one of the two phases. Hong et al. used a similar approach for the large scale preparation of Janus microparticles, with the added advantage that the adsorbed particles were immobilized at the interface by freezing the dispersed phase wax droplets.[44] This method cannot be extended easily to the case where fully water soluble particles need to be prepared, however.

In this work, we present a masking technique that can be used to prepare stable dispersions of Janus nanoparticles in water. Specifically, we adsorb ∼10 nm PAA-coated magnetite nanoparticles onto the surfaces of treated silica beads (∼700 nm), attach polymers to the outer surfaces of these adsorbed nanoparticles to give them properties different from the original PAA coating, and release the Janus nanoparticles from the silica beads by changing the pH. It is shown that these particles can be induced to form small clusters of controlled size when the pH is lowered below the pK_a of the exposed PAA, rendering that portion of the particle surface hydrophobic while the attached polymer remains hydrophilic. This cluster formation is shown to be perfectly reversible. The control of cluster size by changing the molecular weight of the grafted polymer and by mixing Janus nanoparticles with nanoparticles coated only with PAA is discussed. Cryo-TEM imaging is used to visualize the structure of the controlled clusters, and a Monte Carlo model is developed to provide both a qualitative and a semiquantitative interpretation of the observed Janus nanoparticle self-assembly behavior.

(31) Lattuada, M.; Hatton, T. A. *Langmuir* **2007**, *23*, 2158−2168.
(32) Michalet, X.; Pinaud, F. F.; Bentolila, L. A.; Tsay, J. M.; Doose, S.; Li, J. J.; Sundaresan, G.; Wu, A. M.; Gambhir, S. S.; Weiss, S. *Science* **2005**, *307*, 538−544.
(33) Templeton, A. C.; Wuelfing, M. P.; Murray, R. W. *Acc. Chem. Res.* **2000**, *33*, 27−36.
(34) Templeton, A. C.; Hostetler, M. J.; Warmoth, E. K.; Chen, S. W.; Hartshorn, C. M.; Krishnamurthy, V. M.; Forbes, M. D. E.; Murray, R. W. *J. Am. Chem. Soc.* **1998**, *120*, 4845−4849.
(35) Berret, J. F.; Schonbeck, N.; Gazeau, F.; El Kharrat, D.; Sandre, O.; Vacher, A.; Airiau, M. *J. Am. Chem. Soc.* **2006**, *128*, 1755−1761.
(36) Erhardt, R.; Boker, A.; Zettl, H.; Kaya, H.; Pyckhout-Hintzen, W.; Krausch, G.; Abetz, V.; Mueller, A. H. E. *Macromolecules* **2001**, *34*, 1069−1075.
(37) Paunov, V. N.; Cayre, O. J. *Adv. Mater.* **2004**, *16*, 788−791.
(38) Nonomura, Y.; Komura, S.; Tsujii, K. *Langmuir* **2004**, *20*, 11821−11823.
(39) Perro, A.; Reculusa, S.; Ravaine, S.; Bourgeat-Lami, E. B.; Duguet, E. *J. Mater. Chem.* **2005**, *15*, 3745−3760.
(40) Li, Z. F.; Lee, D. Y.; Rubner, M. F.; Cohen, R. E. *Macromolecules* **2005**, *38*, 7876−7879.
(41) Roh, K. H.; Martin, D. C.; Lahann, J. *Nat. Mater.* **2005**, *4*, 759−763.
(42) Perro, A.; Reculusa, S.; Pereira, F.; Delville, M. H.; Mingotaud, C.; Duguet, E.; Bourgeat-Lami, E.; Ravaine, S. *Chem. Commun.* **2005**, 5542−5543.
(43) Nisisako, T.; Torii, T.; Takahashi, T.; Takizawa, Y. *Adv. Mater.* **2006**, *18*, 1152−1156.
(44) Hong, L.; Jiang, S.; Granick, S. *Langmuir* **2006**, *22*, 9495−9499.
(45) Erdmann, T.; Kroger, M.; Hess, S. *Phys. Rev. E* **2003**, *67*, 041209.
(46) Vanakaras, A. G. *Langmuir* **2006**, *22*, 88−93.
(47) Hong, L.; Cacciuto, A.; Luijten, E.; Granick, S. *Nano Lett.* **2006**, *6*, 2510−2514.
(48) Gu, H. W.; Yang, Z. M.; Gao, J. H.; Chang, C. K.; Xu, B. *J. Am. Chem. Soc.* **2005**, *127*, 34−35.

Experimental Section

Materials. 2,2′-Azobis(2-methylpropionamidine)dihydrochloride (97%), benzyl ether (99%), 2-bromo,2-methyl propionyl bromide (BMPB) (98%), copper(I) bromide (CuBr) (98%), 1,2-dichlorobenzene (DCB) (99%), dimethylaminoethyl methacrylate (DMAEMA) (98%), *N*,*N*′-dimethylformamide (DMF) (99.8%), dimethyl sulfoxide (DMSO) (99.6%), 1-ethyl-3-(3-dimethylaminopropyl)carbodiimide hydrochloride (EDC) (97%), iron tri(acetylacetonate) (97%), *N*-hydroxysuccinimide (NHS) (98%), 1,1,4,7,10,10-hexamethyltriethylenetetramine (HMTETA) (97%), *N*,*N*,*N*′,*N*′,*N*′-pentamethyldiethyltrimine (PMDETA) (99%), oleic acid (OA) (90%), oleyl amine (OAm) (70%), potassium bromide (≥99%, IR grade), ricinoleic acid (RA) (80%), 4-styrenesulfonic acid sodium salt hydrate (SSNa) (98%), 1,2-tetradecanediol (90%), tetraethyl orthosilicate (TEOS) (99%), triethylamine (99.9%), 2,2,6,6-tetramethylpiperidine 1-oxyl radical (TEMPO) (>96%), and trimethylsilyl acrylate (TMSA) (98%) were purchased from Sigma Aldrich. Dichloromethane (DCM) (99.97%), diethyl ether (99.9%), hexane (99.9%), and tetrahydrofurane (THF) (99.94%) were purchased from Omisolv. Acetone (99.5%), ammonium hydroxide (35%), ethanol (98%), isopropanol (99%), ethylene glycol (98%), and methanol (99.8%) were purchased from Mellinkrod. *N*-Trimethoxysilylpropyl-*N*,*N*,*N*-trimethylammonium chloride (TMSPTMAC) (50% in ethanol) was purchased from Gelest. All chemicals were used as received. All water utilized in the experiments was Milli-Q (Millipore) deionized water.

(1) Preparation of Oleic Acid-Coated Magnetic Nanoparticles. The procedure followed for the preparation of monodisperse magnetic nanoparticles can be found in Sun et al.[18] Iron tri(acetylacetonate) (2 mmol), 1,2-tetradecanediol (10 mmol), oleic acid (6 mmol), oleylamine (6 mmol), and benzyl ether (20 mL) were mixed and stirred magnetically under a constant flow of nitrogen. The mixture was gradually heated to 100 °C and kept at 100 °C for an overall period of 45 min. A heating rate of 5 °C per min was applied, and 11 nm particles were obtained. Afterward, the mixture was heated to 200 °C for a period of 40 min and kept at 200 °C for 2 h. Finally, under a blanket of nitrogen, the mixture was heated to reflux (∼300 °C) for 1 h. The black-colored mixture was cooled to room temperature by removing the heat source. Methanol (∼40 mL) was added to the mixture, and a black material was precipitated and separated via centrifugation (7000 rpm, 10 min). The black precipitate was dissolved in hexane (20 cm^3) and centrifuged once more (7000 rpm, 10 min) to remove any undispersed residue. The nanoparticles were stored in hexane. Before undergoing any ligand exchange reaction, all particles were precipitated through addition of a large excess of methanol, separated magnetically by means of a powerful electromagnet, and dried in the oven at 80 °C for 20 min to evaporate all alcohol.

(2) Preparation of Ricinoleic Acid-Coated (RA) Magnetic Nanoparticles. 120 mg of oleic acid and oleyl amine-coated nanoparticles prepared as described in step 1 was dispersed in 1,2-dichlorobenzene (15 cm^3) to which 1 g of ricinoleic acid was added. The mixture was then stirred at 80 °C for about 24 h. The particles were subsequently precipitated by addition of methanol (∼40 cm^3) and 2 cm^3 water and recovered by means of an electromagnet. The particles were then dried in a vacuum oven for 20 min at 80 °C.

(3) Preparation of Magnetic Nanoparticles Macroinitiators (RA/BMPB). The nanoparticles subjected to the ligand exchange reaction as described in step 2 were redispersed in dichloromethane (15 cm^3) and stirred vigorously. To this mixture was added 1 cm^3 of triethylamine followed by dropwise addition of 0.5 cm^3 of 2-bromo,2-methylpropionyl bromide. The acylation reaction was allowed to proceed for 3−4 h at room temperature. Particles were then precipitated through addition of acetone and recovered by means of an electromagnet. The particles were subsequently redispersed in acetone and reprecipitated by means of an electromagnet 3−4 times to remove all traces of reagents, followed by 20 min of drying in a vacuum oven at 80 °C.

(4) Preparation of Poly(acrylic acid) (PAA)-Coated Nanoparticles. All of the RA/BMPB magnetic nanoparticles prepared according to the procedure described in step 3 were dissolved in 7.5 cm^3 of DCB and 7.5 cm^3 of DMF inside a three-neck round-bottom flask. To this mixture were added 5 cm^3 of TMSA and 0.11 g of CuBr. After 30 min of N_2 bubbling under vigorous magnetic stirring, 0.4 cm^3 of HMTETA was injected, and the temperature was raised to 90 °C. The reaction was allowed to proceed for 24 h. Finally, the particles were precipitated by adding ∼30 cm^3 of hexane/diethyl ether mixture and recovered by means of an electromagnet. The nanoparticles were then thoroughly washed using methanol and precipitated several times by means of an electromagnet. Subsequently, the nanoparticles were dispersed in methanol and sonicated in a sonicating bath for 1 h to deprotect the polymer and give PAA-coated particles. Particles were then redispersed in 15 cm^3 of H_2O with the help of 0.1 cm^3 of PMDETA. Subsequently, the nanoparticles underwent magnetic filtration to remove larger clusters. At the end, particles were dialyzed against a pH 8 phosphate buffer solution (10 mmol phosphate) for 24 h to remove all impurities.

(5) Preparation of Silica Particles. Silica particles were prepared following the recipe reported by Hsu et al.,[49] which is a slight modification of Stöber's method.[50] Briefly, a mixture of TEOS (0.35 mol/L), NH_3 (1.16 mol/L), H_2O (3.1 mol/L), and isopropanol (0.41 L) was mixed and kept stirring at 45 °C for 1.5 h. The particles so obtained were of size ∼640 nm. At the end of the reaction, the particles were removed by centrifugation and then redispersed in pure water and recentrifuged (this procedure was repeated three to four times).

(6) Silylation of Silica Particles. Two grams of silica particles prepared as described above was dissolved in concentrated HCl aqueous solution (∼6 wt % HCl). The mixture was sonicated for about 60 min, and then the particles were removed by centrifugation. They were subsequently redispersed in pure water and centrifuged out again; this procedure was repeated three or four times to remove all of the acid. Finally, the particles were dried in the oven overnight at a temperature of 80 °C. Next, the silica particles were dispersed in a solution of xylene (40 cm^3) and *N*-trimethoxysilylpropyl-*N*,*N*,*N*-trimethylammonium chloride (TMSPTMAC) (10 cm^3). The mixture was heated to reflux at 140 °C and kept at the same temperature overnight. At the end of the reaction, the particles formed a solid paste-like material in the vessel. The liquid was removed, and the particles were left in a vacuum oven for 36−48 h at ∼140 °C. During this aging process, the bonds between the silylating agent and the particle surface cured. Finally, the particles were suspended in 50 cm^3 of water.

(7) Heteroaggregation between Magnetic Nanoparticles and Silica Particles. 5 cm^3 of the silica particles dispersion prepared as described above was added to 40 cm^3 of deionized water and centrifuged out. The procedure was repeated four times. In this manner, all traces of TMSPTMAC, which lowers the pH of the solution, were removed. Next, the centrifugate was redispersed in 5 cm^3 of aqueous phosphate buffer solution at pH 8. The solution containing silica particles was added dropwise to 5 cm^3 of solution containing PAA magnetic nanoparticles (with a total amount of ∼40 mg of magnetite), under magnetic stirring. Subsequently the mixture was stirred for 3−4 h. Finally, the silica particles coated with magnetite nanoparticles were centrifuged out, redispersed in water (30 cm^3), and centrifuged out again. This procedure was repeated four times. The usually white silica particles developed a brown color when coated with the magnetite nanoparticles. Finally, the magnetic nanoparticle-coated silica particles were redispersed in 10 cm^3 of water.

(8a) Preparation of Amino End-Functionalized PSSNa. To 20 cm^3 of a solution containing a mixture of water and methanol in a 3-to-1 volume ratio was added 20 mmol of SSNa. N_2 was bubbled in the solution for 30 min, and the desired amount of initiator (2,2′-azobis-(2-methylpropionamidine) dihydrochloride) was added through a

(49) Hsu, W. P.; Yu, R. C.; Matijevic, E. *J. Colloid Interface Sci.* **1993**, *156*, 56−65.
(50) Stober, W.; Fink, A.; Bohn, E. *J. Colloid Interface Sci.* **1968**, *26*, 62−69.

syringe. Various amounts of initiator were used to tune the molecular weight of the polymer, always in the range between 0.1 and 0.025 mmol. Next, the temperature of the solution was raised to 60 °C, and the system was stirred for 24 h. The polymer was recovered by precipitation following the addition of a large excess of acetone followed by centrifugation. The centrifuged polymer was dried in a vacuum oven at 80 °C for 24 h and then dispersed in 40 cm^3 of water.

(8b) Preparation of Amino End-Functionalized PSSNa with TEMPO. To 20 cm^3 of a solution containing a mixture of ethylene glycol and water in a 3-to-1 volume ratio were added 20 mmol of SSNa together with the appropriate amount of TEMPO. N_2 was bubbled through the solution for 30 min, and the solution was then heated to 60 °C and stirred for 1 h. The desired amount of initiator (2,2′-azobis-(2-methylpropionamidine) dihydrochloride) was added using a syringe. Various amounts of initiator were used to tune the molecular weight of the polymer, always in the range between 0.1 and 0.025 mmol. The molar ratio between initiator and transfer agent TEMPO was fixed at 1/2. The temperature of the solution was raised to 120 °C, and the system was stirred for 24 h. The polymer was recovered through the addition of a large excess of acetone followed by centrifugation. The centrifuged polymer was dried in a vacuum oven at 80 °C for 24 h.

(8c) Preparation of Amino End-Functionalized PDMAEMA. Twenty mmol of DMAEMA was added to 20 cm^3 of DMF. N_2 was bubbled through the solution for 30 min, and 0.05 mmol of initiator (2,2′-azobis(2-methylpropionamidine) dihydrochloride) was then added via a syringe. The temperature of the solution was raised to 75 °C, and the system was stirred for 24 h. The polymer was recovered through the addition of a large excess of a 0.1 M NaOH water solution. The solution was heated in an oven at a temperature of 60 °C for a few hours. PDMAEMA is insoluble in water at high pH values and at temperatures higher than its lower critical solubility temperature (above ∼50 °C)[51] and precipitates. The precipitated polymer was recovered and dried in a vacuum oven at 80 °C for 24 h.

(9) Anchoring of the Polymer to Magnetite Nanoparticles through Amidation Reaction. To the solution of magnetite-coated silica particles prepared as described in step 7 was added 2 cm^3 of amino end-functionlized polymer, followed by the addition of 0.1 g of EDC and 0.1 g of NHS to promote the amidation reaction between the amino groups of the polymer and the carboxyl groups of the magnetite particles. The mixture was stirred magnetically for 24 h. The particles were then centrifuged out, redispersed in water (30 cm^3), and centrifuged out again (the procedure was repeated three times). Finally, the centrifugate was dispersed in 10 cm^3 of water.

(10) Recovery of the Janus Nanoparticles. Between 0.2 and 0.3 cm^3 of NaOH solution (1 M) was added to the suspension of Janus nanoparticle-coated silica beads prepared in step 10, raising the final pH to ∼12. The mixture was stirred for about 2 h. The silica particles were removed by centrifugation. The Janus nanoparticles that had detached from the silica beads were dispersed in the supernatant, which was then dialyzed against pH 10 solution through a 50 kDa cellulose membrane.

Zeta Potential Measurements. All zeta potential measurements were performed using a Brookhaven ZetaPals Zeta Potential Analyzer (Brookhaven Instruments Corp.). The particles were diluted to 0.1−0.5 wt % of magnetite. The Smoluchowski equation was used to extract the zeta potential ζ from the measured particle electrophoretic mobility μ_e:

$$\zeta = \frac{\eta}{\epsilon}\mu_e \tag{1}$$

where η and ϵ are the viscosity and the dielectric constant of the dispersion medium, respectively. The reported zeta potential values are an average over six measurements, each of which was obtained over 20 electrode cycles. The Smoluchowski equation is only applicable when the particle size is much larger than the Debye length of the electrical double layer in the solution, a condition that was always satisfied in our measurements.

Dynamic Light Scattering Measurements. Dynamic light scattering (DLS) experiments were performed using a Brookhaven BI-200SM light scattering system (Brookhaven Instruments Corp.) at various measurement angles, from 90° to 45°. The autocorrelation function was fit with the cumulant method to extract the average diffusion coefficient, and the Stokes−Einstein equation was used to convert the diffusion coefficient to the hydrodynamic diameter. Samples were measured for 5 min, and measurements were repeated three times to verify the reproducibility of the results.

Transmission Electron Microscopy (TEM). TEM experiments were performed on a JEOL 200CX (200 kV) microscope. All samples were prepared by evaporating dilute suspensions on a 200 mesh carbon-coated film.

Cryogenic Transmission Electron Microscopy (TEM). The vitrified cryo-TEM samples were prepared in a controlled environment vitrification system (CEVS). Thin films of samples were formed by placing a 3−5 μL drop of the liquid on a holey polymer support film that had been coated with carbon and mounted on the surface of a standard TEM grid or a bare 400 mesh copper grid. The drop was then carefully blotted with filter paper until a liquid layer of approximately 50−500 nm in thickness remained across the holes in the support film. About 3−4 s after the liquid film was formed (to allow the system to relax after any shear introduced by the blotting process), it was vitrified by rapidly plunging the holey grid through a synchronous shutter at the bottom of the chamber into liquid ethane (cooled by liquid nitrogen) at its freezing point. The vitrified specimens were mounted on a cryo-transfer stage (Oxford Instruments CT3500J) and examined at 100 kV in the conventional TEM mode of an analytical electron microscope (JEOL 1200EX) equipped with a twin-blade anticontaminator. The specimen temperature was maintained below −165 °C during imaging. The cryo-TEM experiments were performed by Paul Johnson of the University of Rhode Island.

Fourier Transform Infrared (FTIR) Spectroscopy Experiments. FTIR experiments were performed on a Perkin-Elmer 2000 FTIR. Spectra were recorded in the wavenumber interval between 4000 and 400 nm^{-1}. All samples were ground and mixed with KBr and pressed to form pellets. The background spectrum was subtracted from the sample spectrum. Each spectrum was acquired twice, and an average of the two measurements was taken and analyzed.

Thermogravimetric Analysis (TGA). TGA measurements were performed on a Perkin-Elmer TGA7 instrument. All measurements were taken under a constant flow of nitrogen of 50 mL/min. Temperature was increased at a pace of 15 °C/min, starting from room temperature up to 960 °C, and then held constant at maximum temperature for 45 min. All samples were dried in a vacuum oven at 60−80 °C prior to each TGA measurement to remove most of the water or solvent. The initial weight of all samples was between 4 and 20 mg. All reported TGA curves were normalized with respect to the weight at 100 °C to make sure that the solid fraction only was measured.

Monte Carlo Simulations. The Monte Carlo simulation code used in this work is a modified version of an off-lattice cluster−cluster aggregation algorithm used in many investigations in the field of colloidal aggregation and gelation.[52,53] A cubic simulation box with size L is created, and N non-overlapping rigid particles are randomly positioned in this box. The number N is determined by a chosen primary particle volume fraction. In this work, the particle volume fraction was kept fixed at 0.005, and the corresponding number of particles N placed in a box equaled 1838. During every simulation loop, a particle or cluster is chosen randomly with a probability proportional to its

(51) Sen, M.; Sari, M. *Eur. Polym. J.* **2005**, *41*, 1304−1314.

(52) Lattuada, M.; Wu, H.; Morbidelli, M. *J. Colloid Interface Sci.* **2003**, *268*, 106−120.

(53) Lattuada, M.; Wu, H.; Morbidelli, M. *Langmuir* **2004**, *20*, 4355−4362.

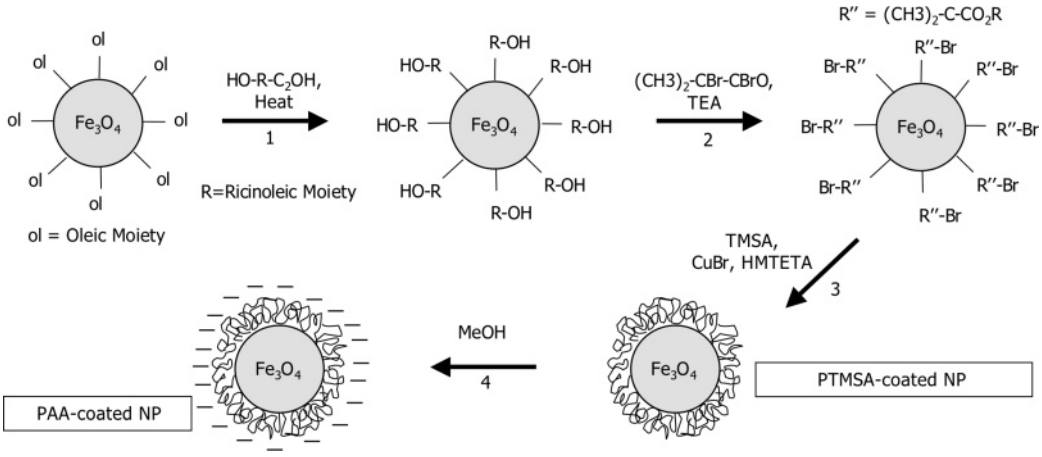

Figure 1. Functionalization of monodisperse magnetic nanoparticles (NP) with PAA.

diffusion coefficient and moved in a random direction over a distance equal to one particle diameter. If the movement leads to a collision with another particle (or cluster), the algorithm evaluates whether the collision fulfills all of the requirements for the formation of a new cluster, and if a positive answer ensues a new cluster is formed with a mass equal to the sum of the masses of the colliding clusters. In case of non-fulfillment of these criteria, the move is discarded. The significant difference between the classical version of the code and the one we have implemented for this work is that, to model the structure of a Janus particle, each spherical primary particle is substituted by a hybrid structure consisting of two interpenetrating non-concentric spheres. The smaller sphere represents the magnetic core, while the larger one (at least the part of it which lies outside the smaller sphere) represents the asymmetrically distributed polymer layer characterizing the particle Janus structure. The direction of the line joining the centers of the two spheres is selected randomly. It is assumed that the surface of the outer, larger sphere represents the charged portion of the nanoparticle surface (i.e., the grafted polymer layer), while the hydrophobic portion of the Janus nanoparticle surface is represented by the free portion of the smallest sphere. Only those collisions occurring between the hydrophobic portions of the surfaces of two colliding Janus nanoparticles are taken to lead to the formation of new clusters, and all other collisions are rejected. A simulation ends either when only one cluster remains in the system, or when a certain predefined simulation time has been reached, depending on which of the two conditions is first met. Both the size ratio of the two spheres and the distance between their centers can be used to tune independently the amount of surface covered by the grafted polymer and the ratio between the polymer layer and solid nanoparticle volumes. The size ratio of the two spheres used in the simulations was set equal to 1.5 consistent with the ratio between DLS measured sizes of Janus and non-Janus nanoparticles. The distance between the centers of the two spheres was varied to probe the effect of changing the relative amount of hydrophobic surface available per particle. The diffusion coefficients of particles and clusters were computed using the Stokes−Einstein equation, and their corresponding hydrodynamic radii were computed using the Kirkwood−Riseman theory.[54,55]

Results and Discussion

Preparation of Janus Nanoparticles. Preparation of PAA-Coated Monodisperse Magnetic Nanoparticles. While several approaches for the preparation of magnetic nanoparticles have been published over the years,[2,3,9,10] the method proposed recently by Sun et al.[18] appears to be particularly attractive as it allows the preparation of fairly monodisperse magnetic nanoparticles with controlled crystallite size, good crystallinity, and, consequently, good magnetic properties. The mixture of oleic acid and oleyl amine adsorbed on the particle surfaces during this synthesis procedure ensures that these particles are well-stabilized in the organic solvents in which they are synthesized, but they provide limited possibilities for further functionalization of the particle surfaces. We have recently described the preparation of PAA-coated magnetic nanoparticles[31] following the procedures summarized in Figure 1. The oleic acid and oleyl amine groups on the nanoparticle surface are replaced through a ligand exchange reaction by ricinoleic acid (step 1 in Figure 1), which has a structure similar to that of oleic acid, and thereby ensures the continued stabilization of the particles in organic suspension. The additional reactive hydroxyl group on this molecule, however, permits effective acylation reactions with, for example, BMPB, to anchor alkyl halide groups on the nanoparticles (step 2 in Figure 1) to serve as ATRP initiators for a surface-initiated living free radical polymerization. This polymerization method allows the growth of a uniform polymer brush directly from the nanoparticle surface, while minimizing the degree of clustering among particles. The ATRP method required that we use a monomer with a protecting group (TMSA), because direct polymerization of acrylic acid-containing monomers interferes with the chain transfer mechanism characteristic of ATRP (step 3 in Figure 1). A simple deprotection step accomplished by suspending the nanoparticles in methanol gave the desired PAA-coated monodisperse nanoparticles[31] (step 4 in Figure 1). A TEM micrograph showing ∼10 nm monodisperse PAA-coated nanoparticles is shown in Figure 2.

Masking of the Nanoparticles. The nonuniform functionalization required to confer Janus-like properties to the PAA-coated nanoparticles can be achieved by masking portions of the nanoparticle surfaces so that they are not available for chemical modification while leaving the exposed surfaces open for the desired functionalization. This procedure has been applied successfully on many occasions,[39] but usually with particles much larger in size than those considered here. For very small particles, but still of size at least an order of magnitude or two greater than the nanoparticles of interest in this work, the masking has been achieved by trapping the particles at the interface between two fluids, such as at air−

(54) Kirkwood, J. G.; Riseman, J. *J. Chem. Phys.* **1948**, *16*, 565−573.
(55) Rotne, J.; Prager, S. *J. Chem. Phys.* **1969**, *50*, 4831−4837.

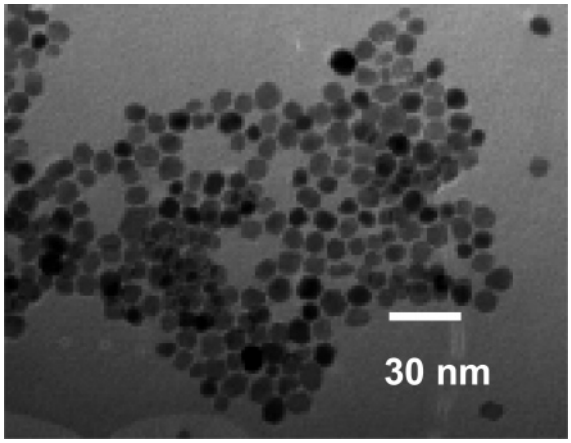

Figure 2. TEM micrograph of PAA-coated, 10 nm magnetite nanoparticles.

water interfaces in a Langmuir trough[56,57] or at the surfaces of emulsion droplets,[44,48] and then chemically modifying the particle surface embedded in one phase but not the other. Recovery of the functionalized particles is a difficult task because of their surface activity, and, although larger particles can be dislodged mechanically from the interfaces by, for example, sonication, small particles must be recovered by other means.

Instead of relying on particle adsorption at a two-fluid interface, we have exploited the electrostatic attachment of negatively charged nanoparticles to the oppositely charged surfaces of sub-micrometer silica beads prepared using the Stöber method,[49,50] as shown schematically in step 2 of Figure 3. The approach is similar to that used for the coating of polystyrene beads with magnetite nanocrystals,[58−60] except that rather than rendering the naturally negatively charged beads positive by the adsorption of a cationic polyelectrolyte, we obtain complete charge reversal on the silica surfaces by silylation[61] with a siloxane containing a positively charged moiety such as a trimethyl ammonium group, as shown in step 1 of Figure 3. The zeta potential of the 640 nm silica beads changed from −52 to +76 mV following silylation and curing of their surfaces.

The degree of adsorption of the PAA-coated magnetite nanoparticles on the positively charged silica beads can be controlled by the solution pH. A well-defined monolayer is deposited on the beads at a pH between 6 and 8, where the PAA-coated nanoparticles are highly charged, as shown in the TEM micrographs of bare and coated silica beads in Figure 4. Such layers are achieved only when a large excess of nanoparticles is used to ensure that the heteroaggregation process is sufficiently rapid that the particles coat the silica beads quickly, before yet-to-be coated, positively charged patches on the silica beads can interact with negatively charged particle-laden patches on other silica beads to induce silica−silica aggregation. The very large size of the silica particles relative to the magnetite nanoparticles (a factor of about 60) favors the diffusion-controlled heteroaggregation process over the much slower bead−bead aggregation.

At a pH of about 4, clusters of incipiently unstable, partially charged PAA-coated nanoparticles form in suspension at the same time as the heteroaggregation process occurs, resulting in the adsorption of clusters and not single nanoparticles on the silica beads. Under these conditions, precise control of the extent of functionalization of the nanoparticle surfaces cannot be obtained, as the fraction of free surface available for subsequent functionalization will vary from nanoparticle to nanoparticle, depending on position within the cluster, leading to a more heterogeneous Janus nanoparticle population. The nonuniformity in the nanoparticle properties is expected to affect their aggregation behavior.

Asymmetric Functionalization of Nanoparticles. We have used polymers and not smaller molecules for the asymmetric functionalization of the nanoparticles, because small molecules might diffuse into the interstices between the silica particle surface and the adsorbed magnetite nanoparticles, negating the advantages of masking one portion of the magnetite nanoparticles. To provide the desired asymmetric particle properties, the polymers were chosen to have different pH responses from that of the PAA that forms the uniform base coating of the magnetite nanoparticles.

The polyanionic polymer PSSNa, which has a practically pH-independent charge density in contrast to the pH-dependent behavior of PAA, was prepared using both conventional free-radical and living free-radical (TEMPO-mediated) polymerization methods, following the procedures developed by Gabaston et al.[62] Living free-radical polymerization allowed for better control of the polymer molecular weight distribution and its impact on the Janus nanoparticle properties. The second polymer used in the preparation of the Janus nanoparticles was PDMAEMA, which is a cationic polymer at low pH, and neutral at high pH values. This polymer resulted in strongly dipolar properties for the Janus nanoparticles under some solution conditions that dictated their aggregation behavior. In all cases, an amino-terminated initiator was used, so that amino end-functionalized polymer chains could be prepared.

The characterization of the polymers, and in particular their average molecular weights, was performed by light scattering with analysis by the Zimm plot method. The values of average molecular weights, together with the average radii of gyration for all polymers, are reported in Table 1. The overall range of molecular weights investigated in this work spans 1 order of magnitude. The average molecular weight of TEMPO PSSNa was typically smaller than that of non-TEMPO PSSNa for the same concentration of initiator used.

All polymers were grafted to nanoparticle surfaces using EDC-mediated amidation reaction (step 3 in Figure 3), because it is characterized by high yields, mild reaction conditions, and easy application in binding many different types of molecules and biomolecules to surfaces.

Recovery of the Janus Nanoparticles. The adsorbed Janus nanoparticles can be separated from the silica beads and recovered by a simple pH change as silica dissolves in both alkaline and acid (HF) solutions with a rate of dissolution that can be controlled by tuning the pH.[63] Because HF dissolves

(56) Petit, L.; Sellier, E.; Duguet, E.; Ravaine, S.; Mingotaud, C. *J. Mater. Chem.* **2000**, *10*, 253−254.
(57) Petit, L.; Manaud, J. P.; Mingotaud, C.; Ravaine, S.; Duguet, E. *Mater. Lett.* **2001**, *51*, 478−484.
(58) Caruso, F.; Susha, A. S.; Giersig, M.; Mohwald, H. *Adv. Mater.* **1999**, *11*, 950−953.
(59) Singh, H.; Laibinis, P. E.; Hatton, T. A. *Langmuir* **2005**, *21*, 11500−11509.
(60) Singh, H.; Laibinis, P. E.; Hatton, T. A. *Nano Lett.* **2005**, *5*, 2149−2154.
(61) Nguyen, V.; Yoshida, W.; Cohen, Y. *J. Appl. Polym Sci.* **2003**, *87*, 300−310.
(62) Gabaston, L. I.; Furlong, S. A.; Jackson, R. A.; Armes, S. P. *Polymer* **1999**, *40*, 4505−4514.

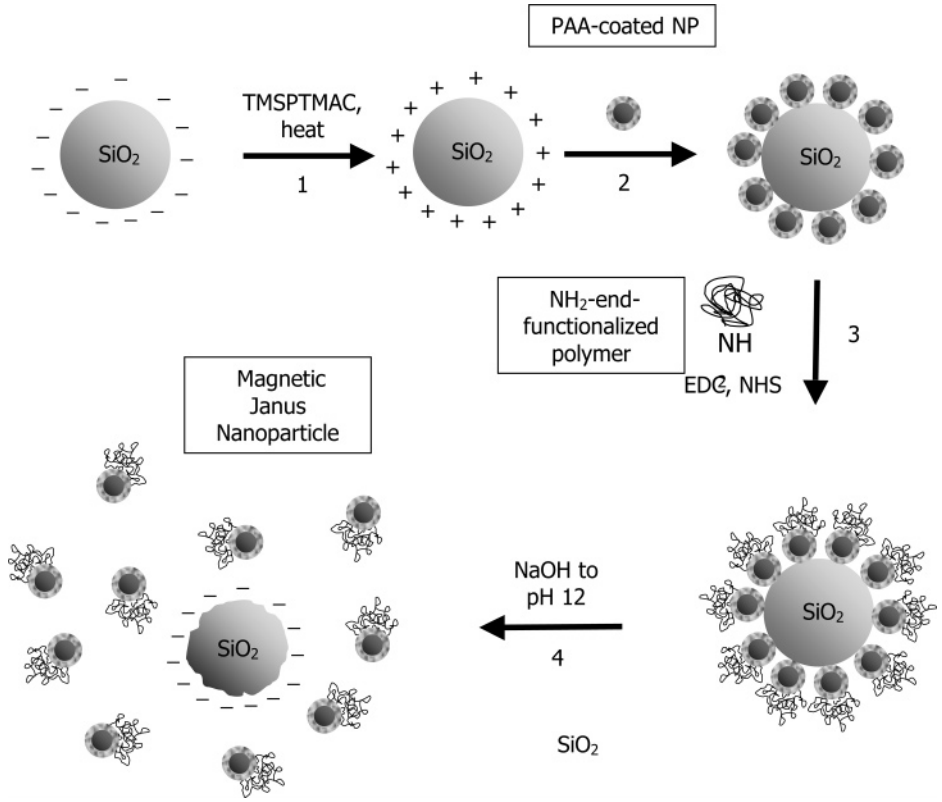

Figure 3. Schematic of masking procedure for the asymmetric functionalization of PAA-coated magnetic nanoparticles (NP).

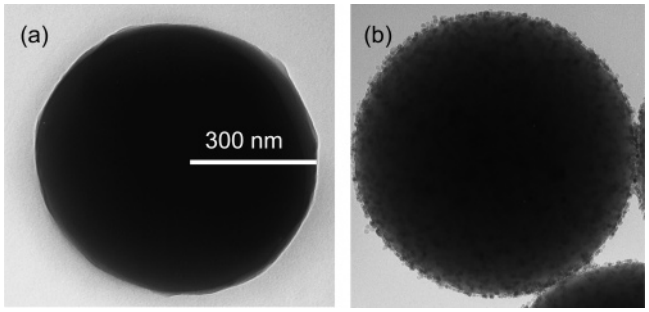

Figure 4. TEM micrographs of (a) a bare 640 nm silica bead and (b) silica beads coated with a monolayer of PAA-coated magnetite nanoparticles.

Table 1. Properties of Polymers Used in the Preparation of Janus Nanoparticles

polymer type	monomer	initiator [mmol]	MW [kDa]	D_g[a] [nm]
1	SSNa	0.05 + 0.1 TEMPO	18.3	9.5
2	SSNa	0.025 + 0.05 TEMPO	23.5	13.2
3	SSNa	0.05	90.8	18.9
4	SSNa	0.025	158	29.6
5	DMAEMA	0.05	91.1	23.2

[a] $D_g = 2R_g$, where R_g is the radius of gyration of the polymer coil in solution.

the magnetite nanoparticles as well as the silica beads, we have restricted our use to an alkaline solution to dissolve the outer silica layers to which the positively charged groups have been attached through silylation (it is not necessary to dissolve the entire silica particle). When positively charged silica particles are immersed in a solution at pH 12 for 1 h, they show a complete surface charge reversal, as indicated by the zeta potential, which changes back to −53 mV, characteristic of the bare silica particles prior to the silylation reaction. This charge reversal leads to a rapid desorption of negatively charged Janus nanoparticles (step 4 in Figure 3). High pH values will also favor dissociation of PAA carboxyl groups and enhance the stability of the Janus nanoparticles. The silica particles are then removed from the suspension by centrifugation.

IR spectra not shown here of PSSNa-coated Janus nanoparticles have absorption bands at wavenumbers between 1400 and 1100, which are indicative of the presence of sulfonate groups; these bands are missing in the spectra for the purely PAA-coated nanoparticles spectra.[64] This further confirms the presence of grafted PSSNa on the Janus nanoparticles.

Controlled Reversible Self-Assembly of Janus Nanoparticles. The self-assembly of the Janus nanoparticles under different solution conditions was tracked by dynamic light scattering (DLS) at 45°, the smallest angle at which a good signal-to-noise ratio could be obtained with clear indications of the size of Janus nanoparticle clusters. The self-assembled samples of these nanoparticles, in particular those with high molecular weight grafted polymers, generally showed a marked increase in the average hydrodynamic radii measured at progressively lower scattering angles, a behavior typical of broad cluster size distributions.

The hydrodynamic diameters obtained for the various PSSNa-coated Janus nanoparticle suspensions at different pH values are shown in Figure 5. At the high pH values at which their entire surfaces were electrically charged and hydrophilic, the coated nanoparticles were dispersed stably as single particles

(63) Iler, R. K. *The Chemistry of Silica: Solubility, Polymerization, Colloid and Surface Properties, and Biochemistry*; Wiley: New York, 1979.

(64) Lin-Vien, D.; Colthup, N. B.; Fateley, W. G.; Grasselli, J. G. *The Handbook of Infrared and Raman Characteristic Frequencies of Organic Molecules*; Academic Press: New York, 1991.

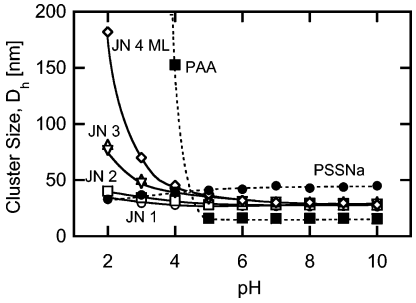

Figure 5. Effect of pH on the average hydrodynamic diameter of different PSSNa Janus nanoparticles (JN indicates Janus nanoparticles; the number refers to polymer type, as given in Table 1; ML refers to nanoparticles functionalized when adsorbed as multilayers), as compared to uniformly PAA-coated nanoparticles and to uniformly PSSNa-coated nanoparticles.

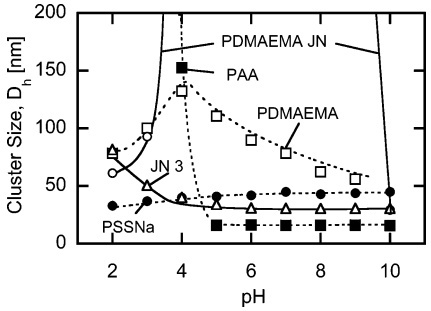

Figure 6. Effect of pH on average hydrodynamic diameter of PDMAEMA and PSSNa (polymer type 3, 90.8 kDa) Janus nanoparticles (JN), and of uniformly PDMAEMA-coated nanoparticles.

with diameters of 23−27 nm, independent of the average molecular weight of the polymer anchored on their surfaces. These results are consistent with the DLS sizes of uncoated particles of ∼15 nm and of free polymer chains of about 10−20 nm (see Table 1). This suggests that the larger is the molecular weight of the polymer, the smaller is the number of chains anchored onto a particle. Controlled aggregation occurs at pH values lower than 5 and is strongly dependent on the molecular weight of the polymer anchored onto the surface. For the lowest MW polymers (∼18.5 kDa), the hydrodynamic size increased by a factor of 1.5 with a decrease in the pH from 10 to 2, while the hydrodynamic diameters increased by factors of 2 and 3 for polymers of molecular weight 23.5 and 90.5 kDa, respectively, clearly indicative of limited and controlled aggregation. The light scattering intensity at 45° increased by only a few times relative to the values obtained for stable, individually dispersed nanoparticles, further supporting the conclusion of a limited growth process. No significant change was detected in most of the samples at pH 2 over a period of about a week. The kinetics of the process were very fast, and, following changes in the pH, the clusters immediately attained sizes close to their final values, with very slight increases in size observed over the next few hours. The clustering was fully reversible: when the pH of the samples was increased back to 10, the aggregation process was reversed and stable particles of the original size were recovered, attributed to the added electrical repulsions as the PAA brushes acquired a charge. Similar behavior has been noted for purely PAA-coated magnetic nanoparticles.[31] This reversibility cannot easily be tested over many cycles, because repeated cycling of the pH leads to an increase in the solution ionic strength, which in the long run leads to screening of inter-particle electrostatic repulsions and destabilization of the particle suspension.

For comparison, Figure 5 also shows the behavior of uniformly coated PSSNa nanoparticles and of PAA-coated nanoparticles. The PSSNa uniformly coated nanoparticles, prepared through ATRP surface-initiated polymerization from aqueous solution, were about twice the size of the Janus nanoparticles, presumably because the polyelectrolyte brush extended from all sides of the nanoparticle surface, rather than just from one side as in the Janus structure. The PAA-coated nanoparticles, on the other hand, were smaller than the Janus nanoparticles at high pH values because the PAA brush was relatively thinner than the attached PSSNa polymer layer. With a decrease in the solution pH, the PSSNa-coated nanoparticles decreased in size, attributed to progressively more screening of the charges on the polyelectrolyte brush with the increasing concentration of H^+ ions, leading to a contraction of the brush itself. In the case of PAA, on the other hand, uncontrolled (but reversible) aggregation was observed as soon as the pH dropped below 5, because the protonated PAA coatings no longer provided the electrostatic stabilization afforded by these polymers at the higher pH values. These results confirmed that the behavior of the Janus nanoparticles, which is intermediate between that of PSSNa- and of PAA-coated nanoparticles, is a result of their hybrid structure.

The PDMAEMA-coated Janus nanoparticles behaved differently from the anionic PSSNa systems, as shown in Figure 6. At very high pH values (larger than 9) the particles were stable, because PDMAEMA is water soluble even though uncharged at room temperature. It is well known that PDMAEMA becomes hydrophobic above a lower critical solubility temperature (LCST), but the hydrophobicity induced by a temperature increase was not sufficient to destabilize particles probably because of the highly charged PAA at these pH values. A similar behavior was observed in our previous study where PNIPAm uniformly coated nanoparticles that were also stabilized by citric acid groups could not be destabilized by simply increasing the temperature of the solution above the LCST of PNIPAm.[31] In the pH range between 9 and 4, the PDMAEMA-coated Janus nanoparticles were completely unstable and precipitated out of suspension. The insolubility is because these Janus nanoparticles are electric dipoles in this pH range, carrying both positive and negative charges, due to the PDMAEMA and PAA polyelectrolytes, respectively. These dipoles aggregate rapidly through favorable Coulombic interactions to form large clusters that precipitate out of suspension. Controlled clustering occurs again at pH below 4; the cluster size at pH 2 is approximately twice that at pH 10, while a larger size is reached at pH 3, probably due to residual dipolar interactions between particles. In these cases, PDMAEMA is highly positively charged, while PAA is practically uncharged and hydrophobic. In contrast, nanoparticles coated uniformly with a very thick layer of PDMAEMA are stable over the entire pH range from 10 to 2. Their change in size with decreasing pH is due first to their acquisition of more charge, which swells the brush, followed by charge screening at lower pH, which leads to a contraction of the brush. As a further confirmation, the zeta potential of PDMAEMA Janus nanoparticles is negative at high pH values (∼ −35 mV) but positive at pH 2 (∼ +30 mV).

It can thus be concluded that the self-assembly of Janus nanoparticles is quite reversible and leads to the formation of stable clusters whose sizes depend on the molecular weight of

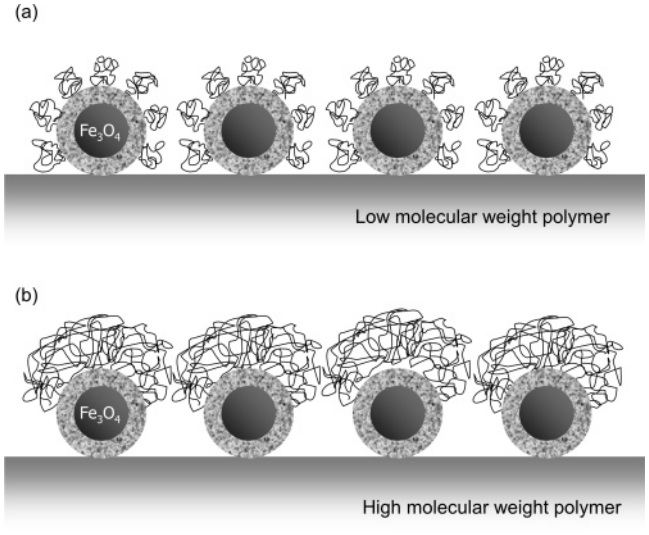

Figure 7. Schematic of polymer molecular weight effects on the formation of Janus nanoparticles with different surface free areas: (a) low MW polymer (with low free surface) and (b) high MW polymer (with high free surface).

the polymer grafted to the underlying PAA shell. The fraction of Janus nanoparticle surface that is coated by the grafted polymer depends on the size of polymer chains, as the schematic in Figure 7 shows. The higher is the polymer molecular weight, the larger will be the size of the random coil, and the larger will be the percentage of surface that will be left uncovered because of the polymer excluded volume. The direct consequence is that with a larger uncovered percentage of the nanoparticle surface the clusters formed by the particles when destabilized will be larger, driven by interactions between the hydrophobic parts of the Janus nanoparticle surfaces. The formation of very small clusters, probably mostly doublets, triplets, and tetramers, will be dominant for low percentages of uncoated surface, while larger clusters can be formed if a smaller portion of the surface is coated, as light scattering results confirm. A more quantitative assessment of this effect will be provided by Monte Carlo simulation results below.

Controlling the Average Cluster Size. It is possible to tune the size of Janus nanoparticle clusters by manipulating the process conditions during the particle synthesis, as indicated above, where the percentage of the Janus nanoparticle surface that was coated with the grafted polymer determined the particle self-assembly behavior. Precise control of the packing of magnetic nanoparticles onto silica spheres, and hence access of the polymer to the surfaces, is difficult to achieve, but we have been able to reduce the amount of polymer on each particle by allowing the heteroaggregation between silica beads and magnetite nanoparticles to occur under low pH conditions. The decrease in solution pH progressively destabilizes the PAA-coated magnetic nanoparticles leading to the formation of clusters of nanoparticles in bulk solution and of a disordered multilayer or collection of fractal clusters of magnetic nanoparticles adsorbed on silica beads instead of just a nanoparticle monolayer. The size obtained by aggregating Janus nanoparticles prepared in this way using a very large molecular weight polymer (type 4; 158 kDa) in combination with a multilayer preparation is shown in Figure 5. It is clear that in this case a 7-fold increase in cluster size as compared to the primary particle size has been achieved. The reason for this substantial increase

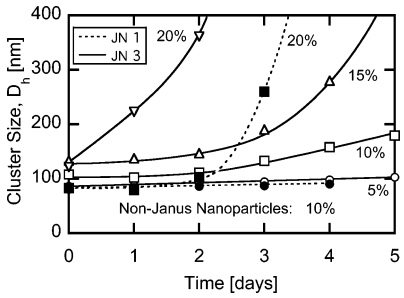

Figure 8. Effect of addition of non-Janus nanoparticles on the growth of Janus nanoparticle aggregates at pH 2. (JN indicates Janus nanoparticles; the number refers to polymer type, as given in Table 1.)

in cluster size is clear: by forming a multilayer of nanoparticles, the percentage of their surface that is available for grafting is on average smaller, giving to the nanoparticles more possibilities to form larger clusters and branched structures when destabilized. It should be noted, however, that for these large clusters a small drift in size was observed for a few days, and did not seem to stop. The size values reported in Figure 5 are the results after 1 week following the destabilization. The fractal dimension of these clusters was determined by static light scattering (SLS) to be 1.4, in agreement with cryo-TEM pictures of the elongated shape of the clusters (see below). Such results could not be obtained for the other samples due to their small size.

Changes in effective surface coverage can be induced in a more controlled manner by using a mixture of Janus nanoparticles with small amounts of PAA-coated (non-Janus) nanoparticles. With this approach the number of particles of each type, and hence the cluster characteristics, can be carefully controlled. The non-Janus nanoparticles offer surfaces upon which the clusters can grow, with many possibilities for branched structures to form. We have prepared suspensions containing type 1 (low MW polymer; 18.3 kDa) or type 3 (high MW polymer; 90.8 kDa) Janus nanoparticles with 5%, 10%, 15%, and 20% of non-Janus nanoparticles. The most significant results are shown in Figure 8. It is observed that for type 1 polymer (18.3 kDa), a steady-state size is achieved with 10% of non-Janus nanoparticle, which is more than twice that of the system with Janus nanoparticles alone. On the other hand, with 20% non-Janus nanoparticles, the clusters are stable only for a day before their growth accelerates and the sample is completely destabilized. In the case of type 3 polymer (90.8 kDa), a steady-state size was reached only for 5% non-Janus nanoparticles in the suspension; this size is 25% larger than that obtained with the pure Janus nanoparticles. No steady state was reached with 10%, 15%, and 20% of non-Janus nanoparticles, and the average hydrodynamic radius drifted slowly toward larger cluster sizes over a few days. Above 10% of non-Janus nanoparticles, the growth accelerated as well, leading to the precipitation of clusters with sizes of several hundreds of particles. The suspension with 10% non-Janus nanoparticles shows a marked drift toward larger sizes, but no irreversible aggregation with precipitation was observed over at least 5 days. Static light scattering on Janus nanoparticles with type 3 polymer and 15% non-Janus nanoparticles 5 days after preparation indicated a cluster fractal dimension of about 2.1, typical of reaction-limited cluster aggregation, and markedly larger than that of pure Janus nanoparticle suspensions.

From these results, it can be inferred that cluster formation is a kinetically driven rather than an equilibrium process, and

reaches a stable size due to the consumption of reactive sites (i.e., hydrophobic part of the Janus nanoparticle surface), which quickly occurs for high degrees of grafting, but might never occur for low degrees of grafting. These conclusions are supported by our Monte Carlo simulations of the nanoparticle self-assembly processes given below.

Monte Carlo Simulations. Recent Monte Carlo simulations have shown that exotic structures may be obtained from the self-assembly of Janus particles with multiple complementary surface patches capable of selectively combining with each other.[45−47] The Janus nanoparticles prepared in this work consist of only two regions, one charged and repulsive, and the other hydrophobic and attractive, and it has been shown that they can aggregate to form simple clusters. The structures to be expected with these types of particles were investigated using Monte Carlo simulations, with the results summarized here.

We have used a modified version of a classic Monte Carlo cluster−cluster aggregation algorithm by treating each Janus nanoparticle as a hybrid structure comprising two interpenetrating, non-concentric spheres, one representing the magnetic nanocrystal core with its hydrophobic surface at low pH conditions, and the other the asymmetric charged polymer layer. Electrostatic interactions between particles were treated implicitly by allowing for a larger steric hindrance of the polymer shell than would be required based on only its physical size. Two Janus nanoparticles were only allowed to stick together if their hydrophobic surfaces came into contact. The various degrees of hydrophobicity of the Janus nanoparticles, which for real particles can be tuned through either a change in the molecular weight of the grafted polymer or by performing the grafting in the presence of particle multilayers on the silica beads, were tuned in the simulations by changing the distance between the centers of the two spheres and their size ratio.

The Monte Carlo simulations confirmed qualitatively the main features of the controlled aggregation of Janus nanoparticles at low pH conditions. The behavior of the system is determined primarily by the fraction of the surfaces that is hydrophobic regardless of sphere size ratios and their center-to-center distances. Thus, in these simulations the size sphere ratio was kept constant at 1.5, while the center-to-center distance was varied to control the percentage of hydrophobic surface. The percentage of hydrophobic surface allowing for the formation of stable clusters was found to be quite small, less than 20%. With more than 30% hydrophobic surface, the aggregation was uncontrolled and the clusters grew without bound.

The Monte Carlo simulations give quite realistic representations of clusters formed under a range of different conditions, as shown in Figure 9, where the simulated clusters are compared to cryo-TEM measurements of the Janus nanoparticle cluster morphologies under low pH conditions. Figure 9a and b shows two images of typical Janus nanoparticle clusters, obtained by rapidly quenching small amounts of pH 2 solutions of type 3 (90.8 kDa) PSSNa-coated (Figure 9a) and PDMAEMA-coated (Figure 9b) Janus nanoparticle suspensions. It is clear that the suspension consists mostly of small clusters, many of them elongated in shape, thus confirming the quite small average sizes measured by DLS.

The most striking feature of these clusters is that there are almost no particles with more than two nearest neighbor particles, in contrast to usual diffusion-limited cluster aggregation where a large percentage of particles have at least three nearest neighbors, and in which branching occurs. These structures are somewhat different from the more compact aggregates predicted by Hong et al.,[47] most likely because of structural differences between the Janus particles in the two simulations. In our Janus nanoparticles, only a small percentage of hydrophobic surface is available for aggregation leading to the growth of only small "snake-like" structures very similar to those observed experimentally in Figure 9. The reason for these structure morphologies is that the steric hindrance provided by the outer spheres (i.e., the repulsive interactions between the charged polymer layers for real Janus nanoparticles) in most cases does not permit more than three hydrophobic surfaces to meet together. As a consequence, the charged parts tend to be positioned on the "outside" part of the cluster, leaving the magnetic cores on the inside. For very low percentages of hydrophobic surface (less than 10%), most of the clusters formed are doublets because when two particles are oppositely oriented and the two hydrophobic surfaces face each other an encounter will very likely prevent any other collision from occurring. Only collisions that involve two particles oriented in such a manner that only the sides of their hydrophobic surfaces can collide will leave enough space for another particle to be accommodated.

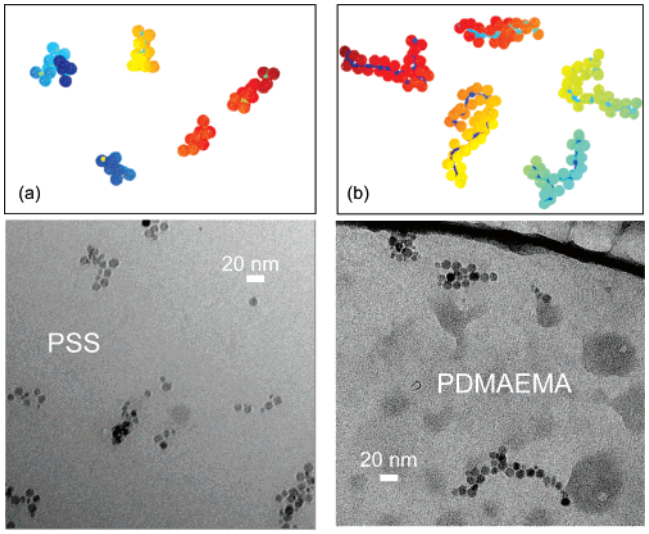

Figure 9. Cryo-TEM micrographs and Monte Carlo simulated clusters of destabilized suspensions of Janus nanoparticles at pH 2 with (a) 90.8 kDa PSSNa and (b) PDMAEMA functionalizations. Both experiments and simulations indicate the formation of elongated clusters. The Monte Carlo simulations were based on a sphere size ratio of 1.5 and a percentage of hydrophobic surface equal to (a) 14.9% and (b) 22.2%.

Figure 10 shows the time evolution of the *z*-average hydrodynamic radius for two different free surface percentages, 8.6% and 22%, simulating approximately the behavior of Janus nanoparticles with type 1 and with type 3 polymers, respectively. In all cases, there is a rapid growth of size in less than a second, followed by either almost no further growth or a progressive slowdown of the growth for low and high percentages of hydrophobic surface, respectively. This absence of growth observed for low percentage of hydrophobic surface is certainly not a thermodynamic equilibrium, but a metastable state in which particles are trapped because as aggregation progresses, the amount of hydrophobic surface still accessible for further growth is progressively reduced. In this steady state, the average hydrodynamic radius is almost double that of the initial particles,

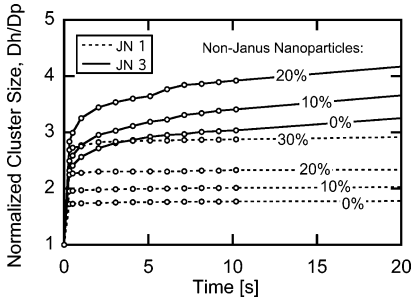

Figure 10. Monte Carlo simulations of the average normalized cluster hydrodynamic diameter D_h (normalized with respect to particle diameter, D_p) growth for Janus nanoparticles of both Janus nanoparticles prepared with 18.3 kDa PSSNa (size ratio 1.5; 8.6% hydrophobic surface; 0%, 10%, 20%, and 30% non-Janus nanoparticle loadings) and 90.8 kDa PSSNa (size ratio 1.5; 22.2% hydrophobic surface; 10% and 20% non-Janus nanoparticle loadings).

in substantial agreement with experimental observations. With slight increases in the percentage of hydrophobic surface to 22%, a 3-fold increase in the average hydrodynamic diameter is achieved and no real steady state seems to be approached during the simulation time.

Monte Carlo simulations also indicate that the addition of non-Janus particles leads to the formation of branch points, such that larger clusters are formed with increasing addition of non-Janus particles. Above a critical concentration of non-Janus particles, the system behavior changes and stable aggregates cannot be found, as shown in Figure 10. Clearly, the larger is the concentration of non-Janus particles, the larger is the size reached in a given time. In addition, for low percentage of hydrophobic surface, even with 20% non-Janus nanoparticles the growth slows substantially, as observed for type 1 polymer (18.3 kDa) Janus nanoparticles. With 22% of the surface being hydrophobic, however, steep growth is observed from the beginning, even with 10% of non-Janus nanoparticles, and is even more pronounced for 20% non-Janus nanoparticles. It should be noted that the sizes reached are close to those observed experimentally. Typical simulated clusters of different sizes and morphologies with different concentrations of non-Janus nanoparticles are shown in Figure 11. Again, the clusters grow as more and more non-Janus nanoparticles are added to the Janus nanoparticle suspension.

On the other hand, the extremely long simulation times (more than 20 h) required to simulate quite short aggregation timescales (a few seconds) do not allow us to follow aggregation behavior over real experimental timescales (several days) and therefore do not allow precise conclusions regarding the long time evolution of the average cluster size. In particular, it is not clear whether the model can account for the observed acceleration in growth rate that occurs after a few days for some samples.

Conclusions

We have described a procedure for the synthesis of asymmetrically functionalized Janus nanoparticles with a final size of about 20 nm that can be induced to form reversible self-assembled structures by changes in solution environmental conditions. Specifically, monolayers of pre-prepared, negatively charged, PAA-coated nanoparticles were adsorbed on the surfaces of sub-micrometer, positively charged silica beads, following which the outer regions of the nanoparticles exposed to the solution were functionalized through the grafting of either

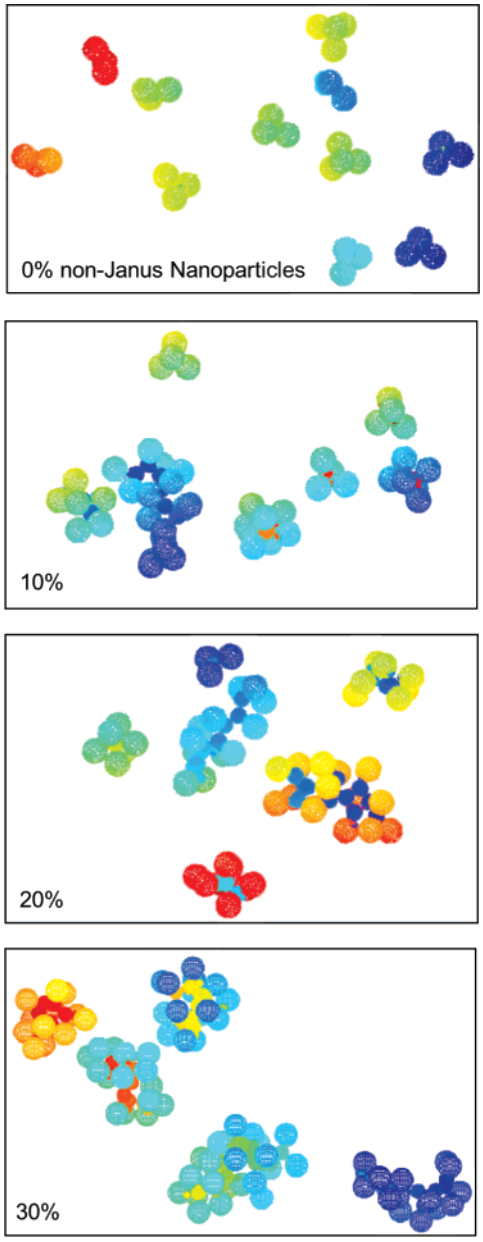

Figure 11. Typical Monte Carlo-generated clusters for Janus nanoparticles prepared with 18.3 kDa PSSNa, with size ratio 1.5, 8.6% hydrophobic surface, and various percentages of non-Janus nanoparticles (0%, 10%, 20%, and 30%).

anionic (PSSNa) or cationic (PDMAEMA) polyelectrolytes. The Janus nanoparticles were released by dissolving part of the silica bead surface and were recovered by centrifugation. The methodologies developed here have been applied to magnetite nanoparticles only, but are sufficiently general that they can readily be extended to the treatment of a wide range of other particle types and geometries. In principle, this approach can be used to prepare large quantities of Janus nanoparticle suspensions, in either batch or continuous mode, as in the work of Hong et al.[47] on the preparation of Janus microparticles using frozen emulsion droplets to anchor the particles for subsequent chemical functionalization.

The PSSNa- and PDMAEMA-functionalized Janus nanoparticles exhibited different clustering behavior with changes in pH, as indicated by dynamic light scattering studies and cryo-

TEM measurements that show the formation of elongated clusters, consistent with the predictions afforded by a qualitative Monte Carlo analysis of such systems. When both polymers on the nanoparticles have the same charge (e.g., PSSNa and PAA at high pH), or when one of them is uncharged but still hydrophilic (e.g., PDMAEMA at high pH), while the other is charged (PAA), then the nanoparticles are dispersed stably as individual entities. When one of the polymers is uncharged and effectively hydrophobic in character (e.g., PAA at low pH) while the other is charged (e.g., either PSSNa or PDMAEMA), finite-sized clusters are formed. When the two polymers bear opposite charges, such as PDMAEMA and PAA at intermediate pH values, uncontrolled aggregation occurs due to the strong dipolar interactions between the Janus nanoparticles. In all cases, self-assembly is reversible, because the original stable particle suspensions can be recovered by increasing the pH of the solution back to high values. The molecular weight of the polymer chains and the efficiency of attachment of these chains to the particles play a significant role in determining their self-assembly behavior and can be used to control the equilibrium cluster sizes. Similarly, the clustering of the Janus nanoparticles can be controlled by adding small amounts of PAA-coated nanoparticles.

This study provides preliminary criteria for the design of Janus nanoparticles for controlled self-assembly applications, but the range of structures formed is still rather limited. We are currently exploring means for generalizing this approach to enable the reversible, directed assembly of structures of a wide range of morphologies, akin to the behavior observed with micellization and solubilization in conventional surfactant systems.

Acknowledgment. The assistance of Szymon Leszczynski in performing some of the experiments is gratefully acknowledged, as is that of Paul Johnson of the University of Rhode Island for carrying out the cryo-TEM study. This work was supported by the DuPont−MIT Alliance.

JA0740521